PERCOLATION THEORY AND ITS APPLICATION IN MATERIALS SCIENCE AND MICROELECTRONICS (Part II – Experiments and numerical simulations)

Andrzej DZIEDZIC

Institute of Microsystem Technology, Wroclaw University of Technology, Poland

Keywords: percolation theory, percolation threshold, applications, materials science, microelectronics, critical exponents, electric conductivity, thermal conductivity, 1/f noise, composite ceramics, electrical thick film resistors, electrical conductive adhesives, VLSI interconnect breakdown, Very Large Scale Integration interconnect breakdown, resistive gas sensors

Abstract: Percolation theory is related to effect of variable range interactions in disordered systems. It permits to characterise the effective properties of such two-phase systems. This paper presents some examples of application of percolation theory in microelectronics and materials science. The following phenomena are discussed: effective conductivity and 1/f noise intensity of model thick-film resistors, the role of dimensional effect on effective transport properties of planar microelectronic structures, percolation model of VLSI interconnect failures, percolative attempt to response of resistive gas sensors, explanation of drug release in the frame of percolation theory.

Teorija perkolacije in njena uporaba v znanosti o materialih in mikroelektroniki (Drugi del - Poskusi in numerične simulacije)

Ključne besede: teorija perkolacije, prag perkolacije, aplikacije, znanost o materialih, mikroelektronika, eksponenti kritični, prevodnost električna, prevodnost toplotna, šum 1/f, keramika kompozitna, upori električni debeloplastni, adhezivi prevodni električno, VLSI preboj povezave vezja integracije zelo visoke stopnje, senzorji plinov uporovni

Povzetek: Teorija perkolacije obravnava efekte interakcij s spremenljivim dosegom v neurejenih sistemih. Omogoča karakterizacijo efektivnih lastnosti takih dvofaznih sistemov. V tem prispevku predstavljam nekaj primerov uporabe teorije perkolacije v mikroelektroniki in znanosti o materialih. Obravnavam naslednje pojave : efektivno prevodnost in gostoto 1/f šuma modelnih debeloplastnih uporov, vlogo dimenzijskih parametrov na efektivne transportne lastnosti planarnih mikroelektronskih struktur, perkolacijski model odpovedi povezav v VLSI vezjih, perkolacijski pristop k obravnavi odziva uporovnih detektorjev plinov in na koncu razlago sproščanja zdravilnih substanc iz zdravil v okviru teorije perkolacije.

Introduction

The percolation problem, which was formulated for the first time in 1957 /1/, is still very attractive and many applications in various areas of basic and applied science convince us about this. The percolation theory is related to effects of variable range interactions in disordered systems. Classical percolation theory describes the effective geometrical and physical properties of random two-phase system but it could be also widened on multipercolative or percolation-like systems /2/. Previous paper /3/ presented percolation phenomenon from theoretical point of view /3/, especially by using of so-called hierarchical model of percolation structure. This paper is dealt with chosen examples of application of percolation theory in microelectronics and materials science. Effective conductivity and effective 1/f noise intensity of model thick-film resistors, the implication of dimensional effects on effective transport properties in planar microstructures, percolation model of VLSI interconnect breakdown, percolative attempt to response of semiconducting oxide gas sensor, and explanation of drug release based on this theory are discussed in more details.

1. Relations resistance – volume fraction of active phase and current noise intensity – volume fraction of active phase in macroscopically disordered composites

Experimental dependence of resistivity ρ (or sheet resistance $R_\square$ in the case of film components) on conductive phase volume fraction v is so-called blending curve. It is commonly used in analysis of electrical properties of composites. Power law (1) fits blending curve very often

$$R_\square = R_0(v\text{-}v_c)^{-t}, \qquad (1)$$

where R_0 - constant, v_c - critical volume fraction of conductive phase, t - critical conductivity exponent above v_c. Therefore sets of optimal v_c and t are looked for various experimental data. Actually Eq. (1) conform to the first constituent of formula (2)

$$\sigma_e = \sigma_1\tau^t(A_0 + A_1 h\tau^{-(t+q)} + \ldots), p > p_c, \tau >> \Delta \qquad (2)$$

well known for percolation structures (usually $h = \sigma_2/\sigma_1 \approx 10^{-15} \div 10^{-20}$; therefore second and higher constituents of

(2) are omitted in most of experimental works). Based on Eq. (1) the experimental data presented in log-log scale should lie near a line with $-t$ slope. Sometimes it is assumed that power law (1) can be applied in the range from percolation threshold p_c and $p_c + 0.2$ /4/.

The v_c and t optimal values for $R_{\square}(v_{CB})$ curves for systems based on high structure (HSCB) or medium structure (MSCB) carbon black are given in Table 1. Moreover Table 2 contains values of v_c and t for other powder filler/organic matrix composites whereas the same parameters for high temperature cermet thick-film resistors are given in Table 3.

Table 1. Values of parameters from Eq. (1) for HSCB/PEI and MSCB/PEI systems cured at various temperatures

T_c [K]	HSCB/PEI system			MSCB/PEI system		
	R_0 [Ω/□]	v_c	t	R_0 [Ω/□]	v_c	t
523	0,070	0	3,110	1,15	0,0737	3,652
573	0,275	0	2,647	7,31	0,0796	2,695
623	0,264	0	2,554	24,27	0,0841	1,755

Table 2. Experimental values of critical volume fraction v_c and conductivity index t for conductive powder filler/organic matrix composites

Conductive powder filler + organic matrix	v_c	t	Ref.
Ketjenblack carbon black (HSCB) + high density polyethylene	0,020	1,9	5
#45 carbon black + high density polyethylene	0,077	1,9	5
Asahi carbon black + high density polyethylene	0,244	2,0	5
Ketjenblack EC300N carbon black + polystyrene	0,002	2,2	6
Graphite (aspect ratio ≅ 100) + epoxy resin $\sigma_{=}$	0,013	2,5	7
Graphite (aspect ratio ≅ 100) + epoxy resin $\sigma_{\perp}$	0,013	2,0	7
Monarch 1100 carbon black (HSCB – 14 nm) + Araldite F resin	0,005	2,0	8
Sterling ST carbon black (LSCB – 300 nm) + Araldite F resin	0,175	1,85	8
Carbon fibre (Φ = 9 μm, l = 1000 μm) + Araldite F resin	0,0093	3,0	8
Carbon fibre (Φ = 9 μm, l = 3000 μm) + Araldite F resin	0,0024	2,9	9
Low structure CB (200 nm) + high density polyethylene	0,170	2,9	10
SAKAP-6 carbon black (MSCB, surface area - 200 m^2/g) + polyesterimide (PEI) resin, T_c = 523 K	0,100	2,415	11
SAKAP-6 carbon black + PEI resin with TiO_2 filler, T_c = 523 K	0,060	2,709	11
Graphite (aspect ratio ≅ 10) + PEI resin, T_c = 523 K	0,140	1,133	11
Graphite (aspect ratio ≅ 10) + PEI resin with TiO_2 filler, T_c = 523 K	0,145	1,461	11
Flammuss101 carbon black + linear low density polyethylene	0,24	1,8	12
Vulcan P carbon black + linear low density polyethylene	0,24	5,0	12
Ag (500 nm) + polystyrene	0,12	1,3	12
Au (1000nm) + polystyrene	0,12	1,8	12
Pd (200 nm) + polystyrene	0,19	2,9	12
Ketjenblack high structure carbon black + polymer	0,0003	2,0±0,2	13

Table 3. Experimental values of critical volume fraction v_c and conductivity index t for high temperature cermet thick resistive film (inorganic matrix - usually lead borosilicate glass)

Conductive phase + inorganic matrix	v_c	t	Ref.
IrO_2 (0,074 μm)* + glass (2 μm), T_f = 973 K	0,052	2,945	14
IrO_2 (0,074 μm) + glass (2 μm), T_f = 1073 K	0,0221	4,716	14
IrO_2 (0,074 μm) + glass (2 μm), T_f = 1148 K	0,0087	4,782	14
RuO_2 (0,010 μm) + glass (0,55 μm)	0,0373	4,01	15
RuO_2 (0,010 μm) + glass (1,60 μm)	0,0237	2,49	16
RuO_2 (0,285 μm) + glass (1,60 μm)	0,0401	5,38	16
RuO_2 (0,040 μm) + glass (0,55 μm)	0,0149	2,10	17
RuO_2 (0,0127 μm) + glass (0,18 μm)	0,0413	2,65	18
RuO_2 (0,170 μm) + glass (0,18 μm)	0,1074	2,87	18
$Pb_2Ru_2O_7$ (0,060 μm) + glass, T_f = 998 K	0	4,5	19
$Pb_2Ru_2O_7$ (0,0058 μm) + glass	0,035	2,796	20
$Pb_2Ru_2O_7$ (0,075 μm) + glass	0,09	2,000	20
$Pb_3Rh_7O_{15}$ (0,040 μm) + glass, T_f = 998 K	0,025	4,1	19
$Bi_2Ru_2O_7$ (0,0047 μm) + glass	0,02	2,04	20
$Bi_2Ru_2O_7$ (0,042 μm) + glass	0,09	1,99	20

Values of R_0 are from the range of tens - several hundred mΩ/sq for HSCB-based system and about two orders larger for MSCB-based one (Table 1). This corresponds with resistivity of about $2,5\times10^{-6}$ and $2,5\times10^{-4}$ Ωm, respectively for nominal thickness of the film equal to 25 μm. Values of R_0 for IrO_2/glass composites are situated between 0.6 and 6 Ω/sq /14/. Increase of curing temperature leads to decrease of conductivity index t. These changes for MSCB/PEI system are much larger than for HSCB/PEI one.

The infinite cluster should appear at $v_c \approx 0.15$ for 3D network /21/ and universal value of conductivity index t should be approximately equal to 2 /2/ in the case of "classical" percolation model (binary distribution of connections, random close package). However, as is shown in Tables 1, 2 and 3, the experimental values of v_c and t are very differentiated and far from universal ones. Some reasons of this fact could be connected with experiment conditions and they are outside the scope of this paper. However there is a question if it is possible to find arguments in percolation theory explaining so various values of v_c and t. And the answer is positive. For example the order function, connected with ratio between spheres representing conductive and insulative phases, is introduced sometimes in 3D discreet lattices. In the case of high-temperature cermet thick film resistor this is the ratio between glass (ϕ) and conductive phase (Φ) mean grain size /22,23/ and the using Monte Carlo simulation one should notice the decrease of v_c from 0.165±0.003 to 0.0197±0.0022 when $\chi = \phi/\Phi$ is increased from 1 to ∞ /15/; the index t is constant. This parameter could be changed in 3D discreet lattice only for multithreshold percolation. For example the RuO_2/glass system with two percolation threshold v_{c1} = 0.1 and v_{c2} = 0.2, i.e. described by equations $R = R_1(v - 0)^{-1,7}$ and $R = R_2(v,1 - 0,2)^{-1,7}$ can be fitted with comparable accuracy by formula $R = R_3(v - 0,1)^{-3,0}$ /18/.

The continuum percolation model (problem of spheres with a_0 characteristic dimension, distributed randomly into the continuous medium of the second phase) is more appropriate when amorphous polymer is used as organic matrix. The distance between such hard spheres can be freely small (not restricted to a_0 scale). Such medium is called SC (Swiss-cheese) or RV (random void) if $v > v_c$ and phase 2 (here ideal insulator) creates random spherical precipitation in continuous phase 1 built from conductive material. The opposite case, i.e. conductive spheres embedded in continuous insulative matrix is called IRV (inverted random void) or ISC /24/. Calculation of critical indices in such models is shown for example in /24/.

The distance between spheres in RV medium is equal to δ ($\delta << a_0$). Therefore using the Weak Link Model /3/ for RV or IRV media we have the bridge consisted of resistors with resistances dependent on δ. The critical conductivity index $\bar{t} = t_{um}$ for IRV and $\bar{t} = t_{um} + 0.5$ for RV model (for 3D medium) has been found when $h(\delta)$ distribution is uniform if $\delta/a_0 \to 0$ /24/. But when we have more general assumption, that

$$h(\delta) \propto \delta^{-\omega} \tag{3}$$

where w is less then 1, then conductivity is described by new, nonuniversal critical index $\bar{t}$ given by Eq. (4)

$$\bar{t} = t_{un} + (u + \omega - 1)/(1 - \omega) \text{ - if } u + \omega > 1$$

and

$$\bar{t} = t_{un} \text{ - if } u + \omega \leq 1, \quad (4)$$

with $u = d - 3/2$ for RV model and $u = d/2 - 1$ for IRV model (d - system dimensionality) /25/. The same percolation theory permits to accept wide range values of t - not only near 2 (characteristic for 3D IRV model) or 2.5 (obligatory for 3D RV model).

The concept of excluded volume, i.e. volume near the object where it is forbidden to put the centre of the other object with similar shape /26/, permits to explain very small values of percolation threshold v_c in continuum percolation model. Percolation threshold is related to total excluded volume $\langle \Omega_{ex} \rangle$, according to formula

$$v_c = 1 - \exp\left(- \frac{\langle \Omega_{ex} \rangle \Omega}{\langle \Omega_e \rangle} \right) = 1 - \exp(- N_c \Omega) \quad (5)$$

where N_c - critical volume density of objects in the medium, Ω - volume of single object, $\langle \Omega_e \rangle$ averaged excluded volume connected with single object and its spatial direction. Value of $\langle \Omega_{ex} \rangle$ is dependent on precipitation geometry. The analysis of excluded volume for cylindrical element with length l and diameter Φ terminated by two identical semispheres (Fig. 1) is given below. It was proved in /26/ that $v_c \propto \Phi/l$ approximately and this explains very small values of percolation threshold.

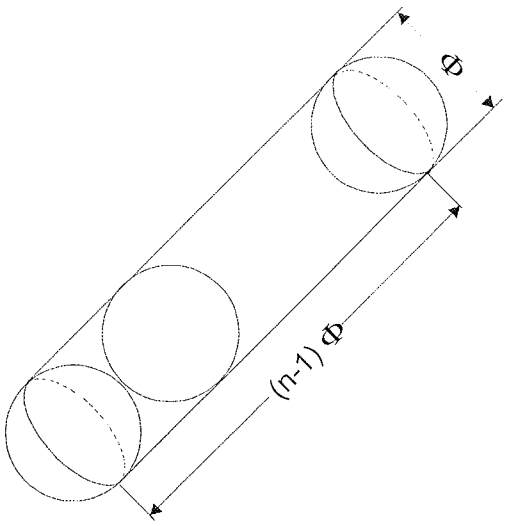

Fig. 1. Cylindrical element composed of carbon black grains in 3D space

Very long chains of individual carbon black grains, kept together by van der Waals forces, are characteristic for high structure carbon black. Replacing such a chain by cylindrical element with $l = n\Phi$ length, where n - number of grains in the chain and Φ - mean diameter of single HSCB grain we get the following equations for Ω and $\langle \Omega_e \rangle$

$$\Omega = \pi \Phi^3 / 6 + \pi \Phi^3 (n - 1)/4 \quad (6)$$

$$\langle \Omega_e \rangle = \frac{4\pi\Phi^3}{3} + 2\pi\Phi^3 (n - 1) + \frac{\pi \Phi^3 (n-1)^2}{2} \quad (7)$$

and the same v_c is given by formula (8)

$$v_c \cong 1 - \exp\left(- \frac{4{,}2}{6n} \right) \quad (8)$$

A few values of v_c are placed in Table 4. It is worth to note that $v_c \approx 0.075$ was found for MSCB-based system (Table 1) and this conform to chain consisting of 10 grains (n = 10).

Table 4. Values of critical volume fraction v_c for medium structure carbon black or high structure carbon black used as active phase (calculated on the basis of Eq. (8))

Type of carbon black	Φ [nm]	n	v_c
MSCB	40	3	0,2081
MSCB	40	10	0,0748
MSCB	40	30	0,0223
HSCB	6	100	$6{,}9\times10^{-3}$
HSCB	6	300	$2{,}3\times10^{-3}$
HSCB	6	1000	$7{,}0\times10^{-4}$
HSCB	6	3000	$2{,}3\times10^{-4}$

It is worth to add that Eq. (1), i.e. one of the basic equations for percolation theory, has been applied successfully in semiquantitative analysis of resistivity changes of polymer thick-film resistors during high hydrostatic pressure compression /27/. The increase of pressure causes decrease of resistor volume. But because of significant compressibility differences between carbon black and polymer the effective volume fraction of conductive phase increases with pressure. This fact leads to such resistance decrease that they are in agreement with Eq. (1).

The noise intensity C versus carbon black volume fraction v_{CB} and curing temperature T_c is shown in Fig. 2. In general it is visible that increase of active phase amount or increase of curing temperature leads to noise intensity decrease.

The below power law

$$C = C_1 (v - v_c)^{-\kappa} \quad (9)$$

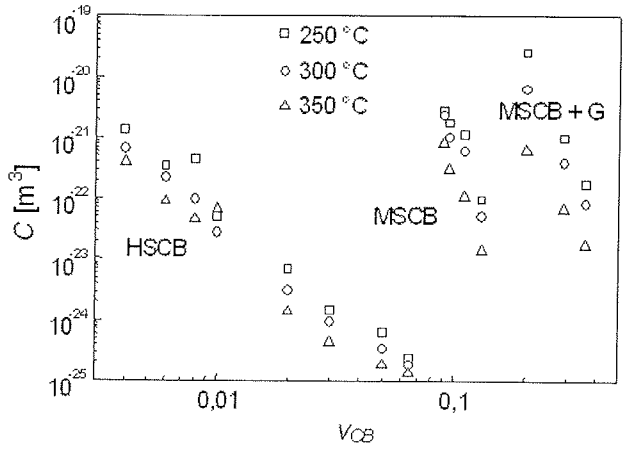

Fig. 2. Noise intensity C versus volume fraction v_{CB} of carbon black (+ graphite for (MSCB+G)-based system) in carbon black/polyesterimide thick-film resistors cured at various temperatures

where C_1 - constant and k - noise critical index is used very often in description of $C(v)$ experimental data. Actually Eq. (9) conform to the first constituent of formula (10)

$$C_e(\tau > 0, \tau >> \Delta) = C_1 \tau^{-k} + C_2 h^2 \tau^{-w} \qquad (10)$$

well known for noise intensity of percolation structures above percolation threshold.

Values of v_c and κ for HSCB/PEI and MSCB/PEI systems are given in Table 5. The C_1 constant is weakly dependent on curing temperature. Kind of active material affects this parameter much stronger - it is about 3 orders smaller for HSCB-based resistors than for MSCB ones. The index κ is decreased when curing temperature is increased. Much larger changes of this parameter are observed for MSCB-based composites.

The dependencies of $R_\square$ as well as C versus volume fraction of active phase are described by power laws (1) and (9), respectively. This is why 1/f noise could be presented in the form of C versus $R_\square$ plot (Fig. 3). This has the advantage that only clearly electrically measurable quantities appear on both axes and the C versus $R_\square$ can be presented as

$$C \propto (R_\square)^\eta \qquad (11)$$

and values of index η for particular investigated carbon/polyesterimide systems and various curing temperatures are shown in Table 6. As has been proven in /29/ continuum percolation theory gives an explanation of $C \propto (R_\square)^\eta$ dependence and observed values of index η. The reader especially interested in index η values both for other polymer as well as high temperature cermet thick-film resistors should find useful information in /29/, too.

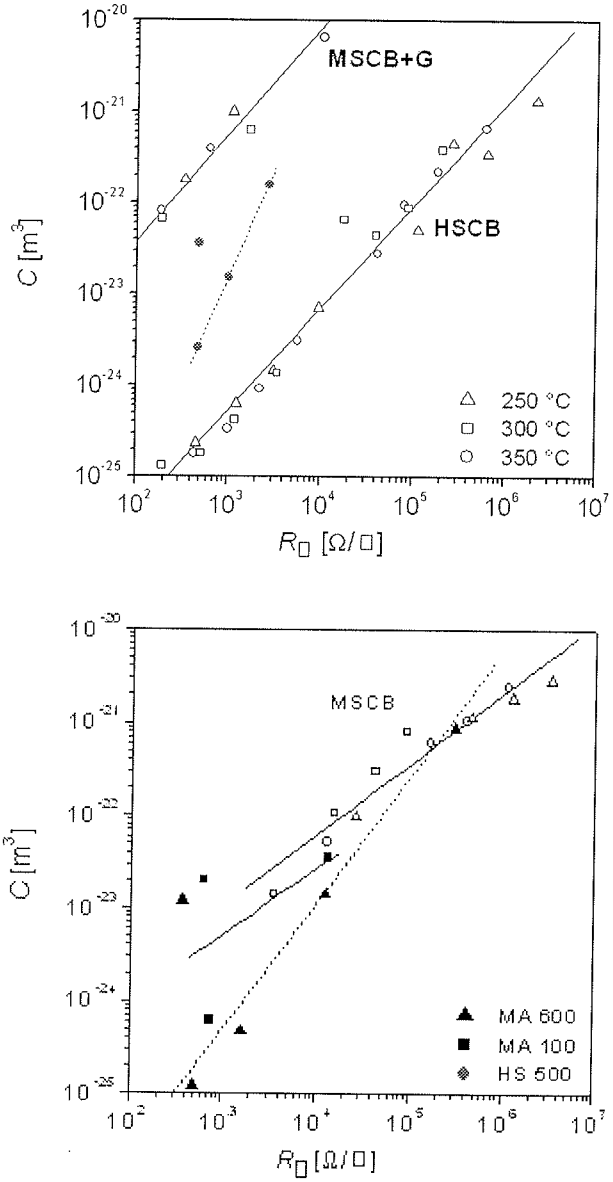

Fig. 3. Noise intensity C versus sheet resistance $R_\square$ for carbon black/polyesterimide (open symbols) and carbon black/polyimide (full symbols - these data refer to results of Fu et al /28/) resistors

Table 5. Variation of Eq. (9) parameters for HSCB/PEI and MSCB/PEI systems cured at various temperatures

T_c [K]	HSCB/PEI system			MSCB/PEI system		
	C_1 [m³]	v_c	κ	C_1 [m³]	v_c	κ
523	$3{,}24 \cdot 10^{-29}$	0	3,200	$2{,}17 \cdot 10^{-26}$	0,0737	3,038
573	$4{,}07 \cdot 10^{-29}$	0	3,035	$1{,}07 \cdot 10^{-25}$	0,0796	2,297
623	$3{,}08 \cdot 10^{-29}$	0	2,980	$8{,}07 \cdot 10^{-26}$	0,0841	2,000

Table 6. Values of index η from $C \propto (R_\square)^{\eta}$ relationship calculated by least square method

System / Curing temperature	HSCB/PEI	MSCB/PEI	(MSCB + G)/PEI
523 K	1,03±0,05	0,83±0,08	1,14±0,09
573 K	1,15±0,03	0,86±0,05	1,07±0,07
623 K	1,17±0,05	1,14±0,05	1,10±0,06

Lets discuss once again so various values of v_c, t and k as have been received from fitting of experimental $R(v)$ and $C(v)$ data for carbon black/polyesterimide composites. Values of v_c and proper constants in Eq. (1) and (9) (R_0 or C_1) are determined in principle by applied active phase. On the other hand curing temperature affects significantly values of critical indices. Similarly as many literature data (please see Table 2 and 3) they do not respond to classical percolation model, where critical exponents depend only are on the dimension of the network and not on its internal structure. So large differences can be explained by very attractive Balberg ideas connected with

- the concept of excluded volume which permits to obtain extremely small values of percolation threshold starting from $v_c \cong 0$,
- modification of system microgeometry by introduction of power distribution of distance between spheres embedded in continuum medium of second phase.

The concept of excluded volume fully explains so significant differences of critical volume fraction in HSCB/PEI and MSCB/PEI systems. But the problem of nonuniversal values of t, κ and $\eta = \kappa/t$ is not so obvious. Nonuniversal value of t can be calculated from Eq. (4). Similarly Balberg /25/ proposed the formula for calculation of nonuniversal value of κ in dependence of universal κ_{un}, system dimensionality d and index ω from Eq. (3).

$$K = \kappa_{un} \text{ for } 2u + z + \omega < 1$$

$$K = \kappa_{un} + (2u + z + \omega - 1)/u \text{ for } 2u + z + \omega \geq 1 \text{ and } u + \omega < 1$$

$$K = \kappa_{un} + (z + 1 - \omega)/(1 - \omega) \text{ for } u + \omega \geq 1, \qquad (12)$$

where d, u, ω as in Eq. (3), $z = d - 1/2$ for RV model and $z = d/2$ for IRV model.

Theoretical shapes of $t(\omega)$, $\kappa(\omega)$ and $\eta(\omega)$ for 3D random void model are shown in Fig. 4. The values of t, κ and η calculated for HSCB/PEI as well as MSCB/PEI systems (Tables 1, 5 and 6) are also placed in Fig. 4. As one could notice the ranges of ω values responding to them are different for particular critical indices. Therefore the problem of nonuniversality of critical indices is still open and application of Balberg conception for interpretation of conductivity and 1/f noise mechanisms needs further verification.

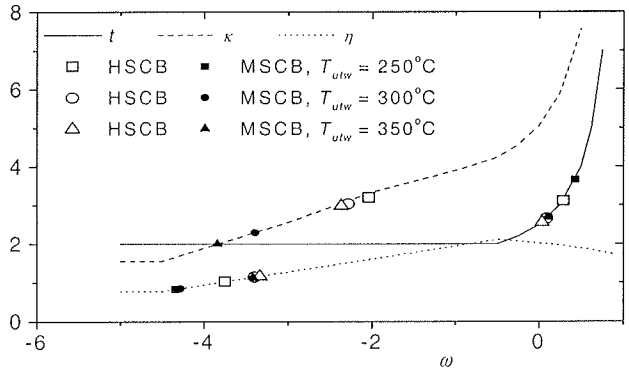

Fig. 4. Dependence of critical exponents t, κ and η in 3D random void model as a function of index ω characterizing the distribution of distances between hard insulating spheres in continuum conductive phase

2. Dimensional effects in percolative systems

Classical model of percolation theory is applied under definite conditions:

- the film should be considered as infinite (with respect to the size of the individual elements),
- the particles have to be spherical, monodispersive and have an isotropic conductivity.

Theoretical, numerical and experimental works have been conducted for cases, when the above assumptions have not been preserved. So far Shklovskii /30/, who considered the critical conductivity behaviour near the percolation threshold in an anisotropic two-component system, and Neimark /31/, who calculated the electrophysical properties of percolation film with a finite thickness, have presented the most formal analyses. But none of papers took into account both finite film thickness and anisotropic shape of fillers, whereas sometimes (for example in conductive adhesive joints) it is necessary to include both matters into theoretical analysis.

Lets consider 3D medium with $L, W, H >> \xi_3$ where L, W, H - length, width and height of structure and ξ_3 - correlation length for 3D system. One should remember that correlation length is the average distance between adjacent nodes and in 3D system

$$\xi_3 \approx a_0 (p - p_{c3})^{-\nu_3} \tag{13}$$

According to standard, two-component percolation model when the concentration of "good" conductors, p (with resistivity ρ_1) exceeds the percolation threshold p_c ($p > p_{c3}$) the effective resistivity

$$\rho_e \approx \rho_1 (p - p_{c3})^{-t_3} \tag{14}$$

where t_3 - universal conductivity index for 3D-system ($t_3 \approx 2$). Theoretical description of film from Fig. 5 ($H < \xi_3$ and $L = W > \xi_3$) demands replacing of initial L x L x H cuboid by set of proper H x H x H cubes.

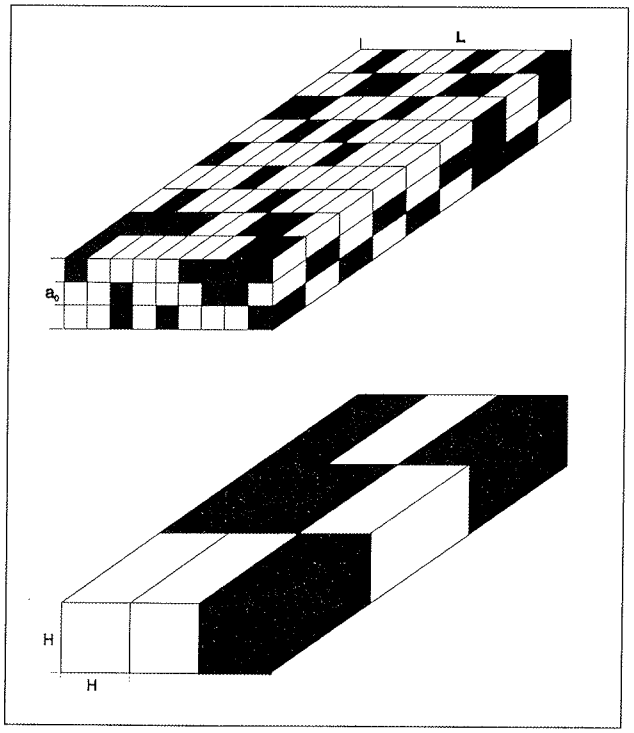

Fig. 5. L x L x H cuboid with percolative structure and equivalent 2D system received as a result of real-space renormalisation procedure

In vertical direction (it corresponds with situation in adhesive joint) all H x H x H cubes are connected in parallel. Knowing the properties of such unit cubes it is possible to apply standard 2D percolation model, where above the percolation threshold ($p > p_{c2}$) the resistance of equivalent 2D system can be expressed as

$$R = r_1 \left(\frac{(p - p_{c2})}{p_{c2}} \right)^{-t_2} \tag{15}$$

and $r_1 = \rho_1 a_0 / a_0^2$, ρ_1 - resistivity of "good" conductor phase ($\rho_1 << \rho_2$), a_0 - the minimal scale of the system under consideration (e.g. the bond length in the case of lattice models).

However for structures with thickness H less than or of the order of correlation length we have so-called fractal (or 2.5D) regime. Modelling of such 2.5D system as 2D system consists in calculation the dependence of r_1 on H. Therefore

$$R_{2.5} = r_1(H) \left(\frac{P_H - p_{c2}}{p_{c2}} \right)^{-t_2} \tag{16}$$

where $R_{2.5}$ - resistance of the film in fractal regime, $r_1(H)$ - resistance of H x H x H cube, P_H - concentration of cubes with $r_1(H)$ resistance, p_{c2} - percolation threshold in 2D system, t_2 - critical conductivity index for 2D system.

This means that for calculation of effective resistance (conductance) in fractal regime it is necessary to know the dependence of $r_i(H)$ and probability of proper conductive realisation. Such a study, showing the critical behaviour of effective conductivity $\{\sigma_e\}$ and effective resistivity $\{\rho_e\}$, averaged over the large numbers of realisation in percolation systems, on the length scale L, has been presented in /32/. Next, the analytical analysis has been widened for systems with weak nonlinearity /33/.

To include the shape of metallic fillers into the model it is assumed that all metallic particles are replaced by ellipsoids. The different shape of real particles (e.g. needles, fibres or flakes) can be projected by different ratios of ellipsoid semiaxes a, b, c (Fig. 6).

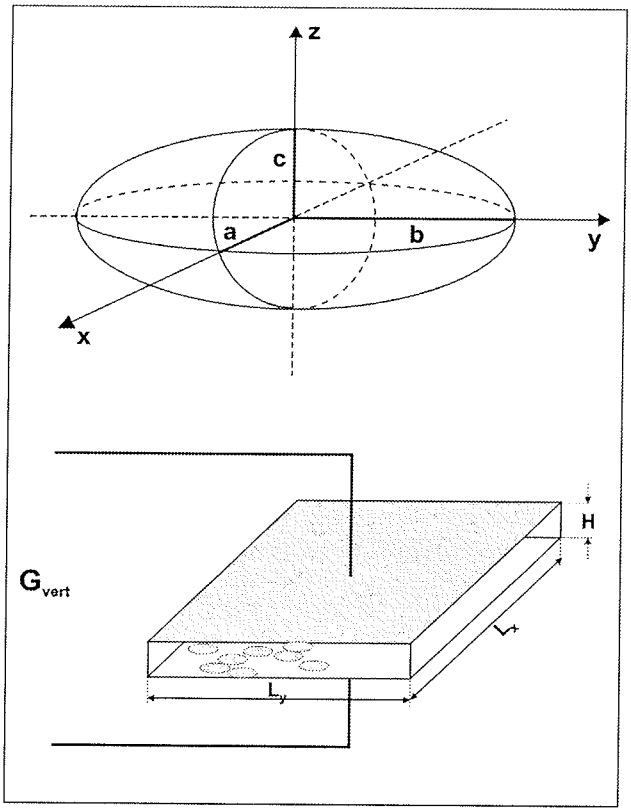

Fig. 6. Shape of ellipsoid representing conductive filler and structure of termination made of isotropically conductive adhesives

Moreover, for model simplicity, it is taken that particles inside termination are monodispersive and their semiaxes are parallel to proper coordinate axes (but their centres are distributed randomly inside the termination volume). According to /32/ the quantity $r_1(H)$ from Eq. (3) is calculated for system within the fractal regime as for percolation system inside smearing region, where this region is described by $\tau_H = (H/c)^{-1/\nu_3}$. Inside τ_H one can meet structures associated with percolation above and below percolation threshold, *i.e.* bridge with resistance R_1 (with probability P_H) and interlayer with resistance R_2 (with probability $1 - P_H$).

Omitting the subsequent stages of calculation and based on /30-33/ we can write the final formula for unit conductance as

$$G_{vert}/L^2 = \alpha^{-2}\sigma_1 c^{(t_3-\nu_3)/\nu_3} H^{-(t_3+\nu_3-1)/\nu_3}\left[(H/c)^{-1/\nu_3}+\tau\right] + \sigma_2 c^{-(q_3+1)/\nu_3} H^{(q_3-\nu_3+1)/\nu_3}\left[(H/c)^{-1/\nu_3}-\tau\right] \quad (17)$$

where $\tau = (p - p_{c3})/p_{c3}$ and parameter of ellipsoid deformation i.e. geometrical anisotropy of conductive grains $\alpha = c/b << 1$

When we are in deeply fractal regime i.e. $(H/c)^{-1/\nu_3} >> |\tau|$ (such situation is characteristic for conductive adhesive joints /34/) we can present the above equation as

$$G_{vert}/L^2 = \sigma_1 \alpha^{-2} \tau_H^{t_3}\left(1 + h\alpha^2 \tau_H^{-\varphi_3}\right) H^{-1} \quad (19)$$

where $h = \sigma_2/\sigma_1 << 1$ and $\varphi_3 = t_3 + q_3$.

Considering the week nonlinearity of both components the unit vertical conductance can be written as

$$\frac{G_z}{L^2} = \left[\frac{\sigma_1}{c}\alpha^{-2}\left(\frac{H}{c}\right)^{-w_1} + \frac{\chi_1}{c^3}\alpha^{-4}\left(\frac{H}{c}\right)^{-w_2}\Delta\phi_H^2\right]\frac{\tau_3+\tau}{\tau_H} + \left[\frac{\sigma_2}{c}\left(\frac{H}{c}\right)^{-w_3} + \frac{\chi_2}{c^3}\alpha^{-4}\left(\frac{H}{c}\right)^{-w_4}\Delta\phi_H^2\right]\frac{\tau_3+\tau}{\tau_H} \quad (20)$$

where $w_1 = (t_3 + \nu_3)/\nu_3$, $w_2 = (3t_3 - \nu_3)/\nu$, $w_3 = w_4 = (\nu_3 - q_3)/\nu_3$, $\Delta\phi_H$ - the voltage drop across the film thickness H and parameter of ellipsoid deformation $\alpha = c/b$.

Based on analogy between voltage susceptibility and noise intensity we have the following formula for effective noise intensity of structure within the fractal region.

$$C_z^e = C_1(H/c)^{(4\nu_3-t_3+1)/\nu_3}\left((H/c)^{-\nu_3}-\tau_3\right) + C_2 h^2\alpha^4(H/c)^{(q_3+2t_3+2\nu_3+1)/\nu_3}\left((H/c)^{-\nu_3}-3\tau_3\right) \quad (21)$$

This formula is valid independently on the ellipsoid shape *i.e.* ratio between ellipsoid semiaxes.

The above equations permit to take into consideration the shape of conductive fillers, ratio between the metal particle sizes and termination geometry, ratio between the conductivity of "good" and "bad" conductors and volume concentration of active phase related to percolation threshold. In order to facilitate numerical simulations it is necessary to know values of three basic universal exponents n (characteristic for system geometry), *t* and *q* (characteristic for conductivity above and below the percolation threshold) both for 2D and 3D systems.

Neimark's analysis and results have been also used by Liang and Li /35/ to study the thermal conductance. They shown, that there exist a thickness effect on thermal conductivity of thin layers of disordered composites (similar to electrical conductivity). For limited layers (*m* - number of layers with unit thickness in vertical (normal) direction) the thermal conductivity in the normal direction is

$$k_{vert} = k_1[p_c + (p - p_c)m^{1/\nu_3}]m^{-t_3/\nu_3} \quad (22)$$

where k_1 is the thermal conductivity of good thermal conducting phase. The thermal conductivity for the in-plane (horizontal) direction is

$$k_{hor} = k_1 m^{(t_2-t_3)/\nu_3}(p - p_c)^{t_2} \quad (23)$$

This means that the thermal conductivity increases in vertical direction with decreasing thickness while the in-plane conductivity declines.

3. Percolation model of metal oxide gas sensors

Metal oxide gas sensors seem be the simplest type chemical sensors - the sensitive layer of these devices consist of a microcrystalline (or nanocrystalline) metal oxide film. Contrary to simple construction the gas detection mechanism is complex, representing interactions between various gaseous molecules and defects at or near surfaces or grain boundaries. It is based on variations of the charge-carrier concentration within a depletion layer at the grain boundaries in the presence of reducing or oxidizing gases, which leads to changes in the height of the energy barriers for free charge carriers. Except of many phenomenological explanations also percolation theory has been applied for analysis of response of gas sensitive-resistors very recently /36,37/.

For example Ulrich *et al* /37/ show that there are transitions between conducting and insulating stage for some nanocrystalline grains of gas-sensitive layer. Such a grain becomes an insulating (is totally exhausted of free charge carriers) when its diameter is below a critical value, Φ_{crit}. They calculate the net number of free electrons from every grain, which can contribute to the conduction process as

$$N_{free} = \frac{4}{3}\pi(\frac{\Phi}{2})^3 n_0 - (N^0_{OXY} - N_{red})$$
$$(4\pi(\frac{\Phi}{2})^2 - f(\Phi, \Phi_{nN}, k)) \quad (24)$$

where n_0 - density of electrons in grain, Φ - grain diameter, N^0_{OXY} - initial surface density of oxygen adsorbed at the grain surface, N_{red} - surface density of chemisorbed gas species and $f(\Phi, \Phi_{nN}, k)$ - function taking into account that after sintering the surface exposed to the ambient atmosphere is smaller than the surface of sphere with diameter Φ (value of function f depends on Φ, diameter of neighbouring grains Φ_{nN} and local coordination number k).

For $N_{free} \leq 0$ grain is insulating, for $N_{free} \geq 1$ is conducting and for $0 \leq N_{free} \leq 1$ the number of free electrons N_{free} should be considered as probability that the grain is conducting. Moreover, according to the percolation theory in order to connect sensor electrodes the concentration of conducting grains must exceed the percolation threshold p_c. This percolation concentration leads to a detection limit. Therefore the variation of conductance and the same the gas sensitivity is very high for concentration of detected gas p just slightly above p_c. As it is seen from Eq. (24) the model of Ulrich *et al* /37/ connects appearing percolation effects of nanocrystalline metal oxide gas sensors with morphology of sensitive layer very strongly.

4. Reliability of VLSI circuits and percolation

It is well known that VLSI chips reliability is determined by the interconnect failure, which consists in the breakdown of the path connectivity. Moreover, the gate oxide breakdown is important in the case of CMOS VLSI circuits. On the other hand much works have been done to explain dielectric or electrical breakdown phenomena of percolative metal-insulator composites (please see for example /38-40/). Therefore it is nothing strange that percolation theory has been applied very recently for reliability analysis of VLSI circuits.

For example a biased percolation model /41-43/ is used for simulation of interconnect failures. Thin-film conductors, which create wire connections between particular transistor structures, can be treated as a large two-dimensional network of identical resistor elements deposited on an insulating substrate with temperature T_0. Because of two different operation modes (constant current and constant voltage) there are two opposite cases when degradation occurs. Single defect corresponds to a zero resistance value of an element (short circuit model) for constant voltage operation mode and to an infinite value of resistor element (open circuit model) for constant current operation mode. The total film degradation is reached when exist one continuous path of defects between lattice contacts.

Therefore the degradation is synonymous with the conductor-insulator transition in open circuit model and conductor-superconductor transition for short circuit model. Moreover the biased percolation model assumes that the degradation starts because of spontaneous creation of some initial defects. When the constant current is applied in such resistor network then the creation of defects causes an increase of the current flowing in the neighbourhood resistors, especially those located in the region perpendicular to the contact direction. Therefore a significant extra Joule heat occurs in this region together with a significant increase of the local temperature.

The mathematical notation is the following

$$W_\alpha = \exp\left(-\frac{E_0}{k_B T_\alpha}\right) \quad (25)$$

where W_a is probability of local defect generation, k_B is the Boltzmann constant, and T_α is the local temperature at the resistor α given by

$$T_\alpha = T_0 + A r_\alpha i_\alpha^2 \quad (26)$$

and A is the key parameter responsible for the coupling between current and device degradation (value of A depends on the heat coupling of each resistor to the substrate), r_α and i_α are the resistance of a single network element and the current flowing in it, respectively. Subsequent evolution stages of biased percolation model and its application (for example to electromigration in metallic lines) one could find in /44-49/.

The breakdown of thin gate oxide layer, which can be defined experimentally as a large increase in conductance, occurs as soon as a critical density of neural electron traps in the oxide is reached. Degraeve *et al* /50/ simulated breakdown of thin SiO_2 layers based on percolation approach and verified such simulations with experimental results. Since the breakdown occurs at a critical electron trap density therefore conduction via generated traps is a plausible breakdown mechanism. This phenomenon has been simulated in the following way:

- a test sample with fixed dimensions has been defined,
- electron traps have been generated at random positions inside this volume,
- a sphere with a fixed radius r has been defined around the generated traps,
- conduction between two neighbouring traps has been possible when their spheres overlapped,
- the breakdown has appeared when a conducting path has been created from one interface (which has been an infinite set of traps) to the other.

Stathis /51/ has modelled oxide breakdown using percolation formalism for very small samples, comparable to the lattice spacing. He shown, that the critical defect density exhibits a strong decrease with thickness below 5 nm, then

becomes constant below 3 nm. For the second value the oxide thickness becomes less than the defect size. Therefore a single defect near the oxide centre is sufficient to create a continuous path across the sample in a 3-nm thickness limit.

5. Application of percolation theory in pharmacy

Many pharmaceutical tablets are composed of binary inert matrices where water-soluble, finely dispersed drugs are embedded in an insoluble carrier material. Such drugs are released in a patient system by diffusion. Percolation theory is a relatively novel approach to design and characterisation of solid dosage forms and controlled drug release properties of such matrix system. Some papers related to this topic (as e.g. /52-57/) one can find in International Journal of Pharmaceutics.

Tablet components usually have quite various electrical properties. For example the difference in electrical conductivity reaches to several orders of magnitude. Therefore the direct resistance measurement of tablets and then resistivity calculation can indicate the presence of percolation threshold /52/. A sudden resistivity drop indicates the presence of infinite clusters of both phases. Moreover such information may provide a valuable tool for explanation of changes observed in dissolution process of matrix tablets. Below the percolation threshold the drug release is incomplete. It has been also proved that so-called "combined percolation threshold" is characteristic for multicomponent tablet systems and therefore they can be reduced to a binary one /54/.

Such a simple experiment and percolation attempt makes easier more rational design of pharmaceutical solid dosage forms. This is an interesting problem in which manner the percolation theory can help to control the drug release properties. Diffusion and conductivity are very similar because both describe transport processes. It is well known from percolation theory that the normal diffusion laws are not valid below the percolation threshold but above p_c the diffusion coefficient D obeys the following power law

$$D = \chi D_0 (p - p_c)^t \qquad (27)$$

where χD_0 represents a scaling factor and t - conductivity exponent /2/. The references /53,57/ confirm both analytically as well as experimentally that tablet's conductivity and dissolution rate process can be successfully modelled by the same basic equation of percolation theory and that both processes scale in an identical way.

6. Conclusions

This paper shows that percolation theory is still alive. As one can notice new problems, for example the role of finite geometry and dimensional effects on the form or characteristic power laws, are solved using novel models of percolation structures. The application range of percolation theory in microelectronics and materials science is very wide. It can be applied in so different areas as reliability of VLSI circuits and novel design concept of pharmaceutical tablets. Of course the presented and discussed examples do not fulfil the problem. Therefore a few subsequent applications, as for ionic composites or for AC transport phenomena in two-phase percolative systems, will be presented in /58/.

Acknowledgement

This work was supported by Polish State Committee for Scientific Research, Grant no 8T11B 055 19

References

/1/ S.R. Broadbent, J.M. Hammersley, Percolation processes. I. Crystals and mazes, Proc. Cambridge Philos. Soc., vol.53 (1957), p.629-641

/2/ D. Stauffer, A. Aharony, Introduction to Percolation Theory, Taylor and Francis, London-Washington, 1992

/3/ A. Dziedzic, A.A. Snarski; Percolation theory and its application in materials science and microelectronics (Part I - Theoretical description), Informacije MIDEM, vol.31 (2001), p.1-9

/4/ S. Kirkpatrick, Percolation and conduction, Rev. Modern Physics, vol.45 (1973), p.574-588

/5/ S. Nakamura, K. Saito, G. Sawa, K. Kitagawa, Percolation threshold of carbon black-polyethylene composites, Jpn. J. Appl. Phys., vol.36 (1997), p.5163-5168

/6/ P. Mandal, A. Neumann, A.G.M. Jansen, P. Wyder, R. Deltour, Temperature and magnetic-field dependence of the resistivity of carbon-black polymer composites, Phys. Rev. B, vol.55 (1997), p.452-456

/7/ A. Celzard, E. Mc Rae, J.F. Mareche, G. Furdin, M. Dufort, C. Deleuze, Composites based on micron-sized exfoliated graphite particles: electrical conduction, critical exponents and anisotropy, J. Phys. Chem. Solids, vol.57 (1996), p.715-718

/8/ F. Carmona, C. Mourey, Temperature-dependent resistivity and conduction mechanism in car-bon particle-filled polymers, J. Mater. Sci., vol.27 (1992), p.1322-1326

/9/ F. Carmona, R. Canet, S. Delhaes, Piezoresistivity of heterogeneous solids, J. Appl. Phys., vol.61 (1987), p.2550-2557

/10/ M.B. Heaney, Measurement and interpretation of nonuniversal critical exponents in disordered conductor-insulator composites, Phys. Rev. B, vol.52 (1995), p.12477-12480

/11/ H. Czarczynska, A. Dziedzic, B.W. Licznerski, M. Łukaszewicz, A. Seweryn, Fabrication and electrical properties of carbon/polyesterimide thick resistive films, Microelectron. J., vol.24 (1993), p.689-696

/12/ J. Kubat, R. Kuzel, I. Krivka, S. Bengston, J. Prokes, O. Stefan, New conductive polymeric systems, Synthetic Metals, vol.54 (1993), p.187-194

/13/ L.J. Adriaanse, H.B. Brom, M.A.J. Michels, J.C.M. Brokken-Zijp, Electron localization in a percolation network: an ESR study of carbon black/polymer composites, Phys. Rev. B, vol.55 (1997), p.9383-9386

/14/ A. Dziedzic, IrO_2-based thick film resistors: manufacturing conditions and percolation, Materials Science, vol.13 (1987), no 3-4, p.199-204

/15/ A. Kusy, Classical percolation threshold and resistance versus temperature behaviour of RuO_2-glass films, Physica B, vol.240 (1997), p.226-241

/16/ A. Szpytma, A. Kusy, On the segregation of the conductive phase in RuO_2-based thick resistive films, Thin Solid Films, vol.121 (1984), p.263-270

/17/ K. Bobran, A. Kusy, An experimental verification of a percolation model for RuO_2-glass thick resistive films, J. Phys.: Condens. Matter, vol.3 (1991), p.7015-7026

/18/ S.F. Carcia, A. Suna, W.D. Childers, Electrical conduction and strain sensitivity in RuO_2 thick film resistors, J. Appl. Phys., vol.54 (1983), p.6002-6008

/19/ W.H. De Jeu, R.W.J. Geuskens, G.E. Pike, Conduction mechanisms and 1/f noise in thick-film resistors with $Pb_3Rh_7O_{15}$ and $Pb_2Ru_2O_7$, J. Appl. Phys., vol.52 (1981), p.4128-4134

/20/ S.F. Carcia, A. Ferretti, A. Suna, Particle size effects in thick film resistors, J. Appl. Phys., vol.53 (1982), p.5282-5288

/21/ R. Zallen, The physics of amorphous solids, John Wiley and Sons, 1983

/22/ P.J.S. Ewen, J.M. Robertson, A percolation model of conduction in segregated systems of metallic and insulating materials: application to thick film resistors, J. Phys. D: Appl. Phys., vol.14 (1981), p.2253-2268

/23/ E. Listkiewicz, A. Kusy, Computer simulation of thick resistive films as two-component percolation systems: segregation of the conducting component, Thin Solid Films, vol.130 (1985), p.1-15

/24/ S. Feng, B.I. Halperin, P.N. Sen, Transport properties of continuum systems near percolation threshold, Phys. Rev. B, vol.35 (1987), p.197-214

/25/ I. Balberg, Limits of the continuum-percolation transport exponents, Phys. Rev. B, vol.57 (1998), p.13351-13354

/26/ I. Balberg, Recent developments in continuum percolation, Phil. Mag. B, vol.56 (1987), s.991-1003

/27/ A. Dziedzic, A. Magiera, R. Wisniewski; Hydrostatic high pressure studies of polymer thick-film resistors, Microelectronics Reliability, vol.38 (1998), p.1893-1898

/28/ S.-L. Fu, M.-S. Liang, T. Shiramatsu, T.-S. Wu, Electrical characteristics of polymer thick film resistors, Part I: Experimental results, IEEE Trans. on Comp., Hybr., and Manuf. Technol., vol. CHMT-4 (1981), p.283-288

/29/ A. Dziedzic, A. Kolek, 1/f noise in polymer thick-film resistors, J. Phys. D: Appl. Phys., vol.31 (1998), p.2091-2097

/30/ B.I. Shklovskii, Anisotropy of percolation conduction, Physica Status Solidi (b), vol. 85 (1978), p.K111-K114

/31/ A.V. Neimark, Electrophysical properties of a finite thickness percolation layer, Sov. Phys. JETP, vol. 91 (1990), p.341-349

/32/ A.E. Morozovskii, A.A. Snarskii, Finite scaling of the effective conductivity in percolation systems with nonzero ratio of the phase conductivities, J. Experimental and Theoretical Physics, vol. 82 (1996), p.361-365

/33/ A. Dziedzic, A.A. Snarskii, S.I. Buda; Nonlinear properties of two-phase composite films with a fractal structure, Technical Physics, vol.45 (2000), p.334-338

/34/ A. Dziedzic, A.A. Snarskii, S.I. Buda, K.V. Slipchenko; Percolation study of isotropically conductive adhesives, Proc. 22nd Int. Spring Seminar on Electronics Technology, Dresden-Freital (Germany), May 1999, p.6-10

/35/ X.-G. Liang, X. Ji, Thermal conductance of randomly oriented composites of thin layers, Int. J. of Heat and Mass Transfer, vol.43 (2000), p.3633-3640

/36/ D.E. Williams, K.F.E. Pratt, Microstructure effects on the response of gas-sensitive resistors based on semiconducting oxides, Sensors and Actuators B, vol.B70 (2000), p.214-221

/37/ M. Ulrich, C.-D. Kohl, A. Bunde, Percolation model of a nanocrystalline gas sensitive layer, Thin Solid Films, vol. 391 (2001), p.299-302

/38/ P.O. Jansson, G. Grimvall, Joule heat distribution in disordered resistor networks, J. Phys. D: Appl. Phys., vol.18 (1985), p.893-900

/39/ M. Soderberg, Resistive breakdown of inhomogeneous media, Phys. Rev. B, vol.35 (1987), p.352-357

/40/ Y. Yagil, G. Deutscher, D.J. Bergman, The role of microgeometry in the electrical breakdown of metal-insulator mixtures, Int. J. Modern Physics B, vol.7 (1993), p.3353-3374

/41/ Z. Gingl, C. Pennetta, L.B. Kiss, L. Reggiani, Biased percolation and abrupt failure of electronic devices, Semicond. Sci. Technol., vol.11 (1996), p.1770-1775

/42/ C. Pennetta, Z. Gingl, L.B. Kiss, L. Reggiani, Biased percolation and electrical breakdown, Semicond. Sci. Technol., vol.12 (1997), p.1057-1063

/43/ C. Pennetta, Z. Gingl, L.B. Kiss, L. Reggiani, M. De Vittorio, A. Cola, M. Mazzer, A percolative simulation of dielectric-like breakdown, Microelectron. Reliab., vol.38 (1998), p.249-253

/44/ C. Pennetta, L. Reggiani, L.B. Kiss, Thermal effects on the electrical degradation of thin film resistors, Physica A, vol.266 (1999), p.214-217

/45/ C. Pennetta, L. Reggiani, Gy. Trefan, Scaling and universality in electrical failure of thin films, Phys. Rev. Lett., vol.84 (2000), p.5006-5009

/46/ C. Pennetta, Gy. Trefan, L. Reggiani, Scaling law of resistance fluctuations in stationary random resistor networks, Phys. Rev. Lett., vol.85 (2000), p.5238-5241

/47/ C. Pennetta, L. Reggiani, Gy. Trefan, A percolative approach to reliability of thin films, IEEE Trans. on Electron Devices, vol.47 (2000), p.1986-1991

/48/ C. Pennetta, L. Reggiani, Gy. Trefan, F. Fantini, I. De Munari, A. Scorzoni, A percolative simulation of electromigration phenomena, Microelectronic Engineering, vol. 55 (2001), p.349-355

/49/ C. Pennetta, L. Reggiani, Gy. Trefan, F. Fantini, A. Scorzoni, I. De Munari, A percolative simulation to electromigration in metallic lines, J. Phys. D: Appl. Phys., vol.34 (2001), p.1421-1429

/50/ R. Degraeve, G. Groeseneken, R. Bellens, J.L. Ogier, M. Depas, P.J. Roussel, H.E. Maes, New insights in the relation between electrical trap generation and the statistical properties of oxide breakdown, IEEE Trans. on Electron Devices, vol.45 (1998), p.904-911

/51/ J.H. Stathis, Percolation models for gate oxide breakdown, J. Appl. Phys., vol.86 (1999), p.5757-5766

/52/ M.J. Fernandez-Hervas, M.T. Vela, M.A. Holgado, J. del Cerro, A.M. Rabasco, Determination of percolation thresholds in matrix-type controlled release systems: application of a resistance analysis technique, Int. J. Pharmaceutics, vol.113 (1995), p.39-45

/53/ H. Leutenberger, J.D. Bonny, M. Kolb, Percolation effects in matrix-type controlled drug release systems, Int. J. Pharmaceutics, vol.115 (1995), p.217-224

/54/ I. Caraballo, M. Fernandez-Arevalo, M. Millan, A.M. Rabasco, H. Leutenberger, Study of percolation thresholds in ternary tablets, Int. J. Pharmaceutics, vol.139 (1996), p.177-186

/55/ L.M. Melgoza, I. Caraballo, J. Alvarez-Fuentes, M. Millan, A.M. Rabasco, Study of morphine hydrochloride percolation thresh-

old in EudragitŇRS - PM matrices, Int. J. Pharmaceutics, vol.170 (1998), p.169-177

/56/ M.C. Soriano, I. Caraballo, M. Millan, R.T. Pinero, L.M. Mengoza, A.M. Rabasco, Influence of two different types of excipient on drug percolation threshold, Int. J. Pharmaceutics, vol.174 (1999), p.63-69

/57/ Ch. Siegmunt, H. Leuenberger, Percolation theory, conductivity and dissolution of hydrophilic suppository bases (PEG systems), Int. J. Pharmaceutics, vol.189 (1999), p.187-196

/58/ A. Dziedzic, Some remarks about application of percolation theory in microelectronics and materials science, 37th Int. Con. on Microelectronics, Devices and Materials, MIMED 2001, Bohinj (Slovenia), Oct. 2001 (to be presented)

Andrzej DZIEDZIC
Institute of Microsystem Technology,
Wroclaw University of Technology,
Wybrzeze Wyspianskiego 27,
50-370 Wroclaw, Poland,
e-mail: adziedzic@pwr.wroc.pl

Prispelo (Arrived): 09.07.2001 *Sprejeto (Accepted): 20.08.2001*